

Effect of the Length of a Torpedo Anchor on Its Vertical Holding Capacity

by

John Voon Hsien Yoong

16034

Dissertation submitted in partial fulfilment of
the requirements for the
Bachelor of Engineering (Hons)
Mechanical Engineering

JANUARY 2016

Universiti Teknologi PETRONAS
Bandar Seri Iskandar
31750 Tronoh
Perak Darul Ridzuan

CERTIFICATION OF APPROVAL

**Effect of the Length of a Torpedo Anchor on Its Vertical Holding
Capacity**

by

John Voon Hsien Yoong

16034

A project dissertation submitted to the
Mechanical Engineering Programme
Universiti Teknologi PETRONAS
in partial fulfilment of the requirement for the
BACHELOR OF ENGINEERING (Hons)
MECHANICAL ENGINEERING

Approved by,

(Dr. William Pao King Soon)

UNIVERSITI TEKNOLOGI PETRONAS
TRONOH, PERAK
JANUARY 2016

CERTIFICATION OF ORIGINALITY

This is to certify that I am responsible for the work submitted in this project, that the original work is my own except as specified in the reference and acknowledgements, and that the original work contained herein have not been undertaken or done by unspecified sources or persons.

(JOHN VOON HSIEN YOONG)

ABSTRACT

Since its introduction in 1996, the torpedo anchor has built a reputation for itself as a simple and cost effective deepwater anchoring solution. While numerous field tests and numerical research has been done to verify the torpedo anchors holding capacity under various load and soil conditions, the effect of the geometry of the anchor itself on its holding capacity has not been properly identified. This research attempts to improve the database of knowledge regarding the torpedo anchor. Specifically, the research objectives are i) to evaluate the vertical holding capacity of torpedo anchors using analytical and numerical methods and ii) to analyze the correlation between the total length of a torpedo anchor and its vertical holding capacity. The numerical method uses a 2-D axisymmetric model to evaluate the vertical holding capacity with respect to varying total lengths. Both the soil and anchor were simulated as homogeneous, isotropic linearly elastic materials using plane elements capable of demonstrating non-linearity and large displacement behaviour. The non-linear interaction between the anchor and soil is also modelled using contact finite elements that allow relative sliding and detachment between the two surfaces in contact. Results from the numerical analysis is compared with analytical calculations using a variation of the ultimate load bearing capacity equation for conventional piles to suit the use for torpedo anchors. The pattern of results obtained from both the numerical model and the analytical calculations agreed upon the premise that the vertical holding capacity of a torpedo anchor increases as the total length of the anchor increases.

ACKNOWLEDGEMENTS

First and foremost, I would like to express my utmost gratitude to my supervisor Dr. William Pao for allowing me to undertake my Final Year Project under your supervision and for all your motivational words and patience for me.

I would like to express my sincere thanks to Mr. Abdallelah Ganawa for taking time out of your hectic schedule to advise me regarding finite element simulation.

Thank you also to my all colleagues for making yourselves available whenever I needed some help or advice.

Last but not least, I would like to express my perpetual gratitude to my parents for granting me this opportunity to learn and experience all that I have throughout my years in Universiti Teknologi PETRONAS.

I also place on the record, my sense of gratitude to one and all, who directly or indirectly, have lent their hand in the completion of this project.

LIST OF FIGURES

- Figure 2.1: Suction pile with taut leg mooring
- Figure 2.2: Schematic of Vryhof Stevmanta (left) and Anchor drag installation (right)
- Figure 2.3: Schematic of SEPLA installation
- Figure 2.4: Full scale torpedo pile and releasing situation
- Figure 2.5: Model B (left) and Model N (right) used in centrifuge test
- Figure 2.6: Direction of load applied to the anchor and the two planes used to measure effect of load inclination with respect to fluke planes
- Figure 2.7: Load and reaction forces a pile
- Figure 3.1: Flow of project tasks
- Figure 3.2: Schematic representation of the torpedo anchor and its relevant dimensions
- Figure 3.3: Schematic of FE model
- Figure 3.4: Area of soil body (left) and constraints applied onto soil body (right)
- Figure 4.1: Graph of vertical holding capacity versus total length of torpedo anchor
- Figure 4.2: Graph of load resistance versus total length of torpedo anchor
- Figure 4.3: Graph of surface area versus total length of torpedo anchor
- Figure 4.4: Stress-strain curve of an isotropic linear elastic material
- Figure 4.5: Soil-anchor model (left) and Von Mises stress contours after gravity load (right)
- Figure 4.6: Shear stress contours (left) and contact status (right) of the 15m length anchor model at 3.53MN load
- Figure 4.7: Graph of vertical holding capacity versus total length of torpedo anchor for FE model and analytical calculations

LIST OF TABLES

- Table 3.1: Relevant parameters used in analytical calculation of torpedo anchor holding capacity
- Table 3.2: Properties of soil model
- Table 3.3: Properties of anchor model

ABBREVIATIONS AND NOMENCLATURE

A_p	= area of pile tip
A_{tip}	= tip area of torpedo anchor
A_{wall}	= wall area of torpedo anchor
B	= width of foundation
c'	= cohesion of the soil supporting the pile tip
c_u	= undrained cohesion of the soil below pile tip
D	= diameter of torpedo anchor
D_p	= pile width
f	= unit friction resistance at any depth z
L_{total}	= total length of torpedo anchor
L_1	= length of torpedo anchor body
L_2	= length of torpedo anchor tip
$N_c, N_c^*, N_q^*, N_\gamma^*$	= bearing capacity factors
p	= perimeter of the pile section
p'_o	= overburden pressure at torpedo anchor mid-length
q	= vertical stress
q_{av}	= average unit tip resistance of torpedo anchor
q'	= effective vertical stress
q_p	= unit point resistance
q_u	= ultimate bearing capacity
Q_f	= friction resistance of torpedo anchor
Q_p	= pile ultimate load-carrying capacity
Q_{tip}	= tip resistance of torpedo anchor
Q_v	= vertical pullout/holding capacity of torpedo anchor
s_u	= undrained shear strength of soil
W'	= submerged weight of torpedo anchor
α	= adhesion of soil
γ	= unit weight of soil
ΔL	= incremental pile length over which p and f are taken constant
τ_{vn}	= unit soil friction

TABLE OF CONTENTS

ABSTRACT.....	i
ACKNOWLEDGEMENTS	ii
LIST OF FIGURES	iii
LIST OF TABLES	iii
ABBREVIATIONS AND NOMENCLATURE.....	iv
TABLE OF CONTENTS.....	v
CHAPTER 1: INTRODUCTION	1
1.1 PROJECT BACKGROUND.....	1
1.2 PROBLEM STATEMENT	2
1.3 OBJECTIVE	2
1.4 SCOPE OF STUDY	2
CHAPTER 2: LITERATURE REVIEW	3
2.1 SUCTION PILES/ANCHORS	3
2.2 VERTICALLY LOADED ANCHORS (VLA)	4
2.3 SUCTION EMBEDDED PLATE ANCHOR (SEPLA)	6
2.4 TORPEDO ANCHORS	7
2.5 LOAD BEARING CAPACITY OF PILES	10
CHAPTER 3: METHODOLOGY	14
3.1 PROJECT WORK & FLOWCHART.....	14
3.2 ANALYTICAL CALCULATIONS	15
3.3 FINITE ELEMENT (FE) MODELING.....	17
3.4 GANTT CHART.....	21
CHAPTER 4: RESULTS AND DISCUSSION.....	22
4.1 ANALYTICAL CALCULATIONS	22
4.2 FINITE ELEMENT (FE) MODELING.....	25
CHAPTER 5: CONCLUSION AND RECOMMENDATION.....	29
REFERENCES.....	30

CHAPTER 1

INTRODUCTION

1.1 PROJECT BACKGROUND

The rise to prominence of deepwater oil and gas exploration and production (E&P) from a state of obscurity to becoming a major consideration in the petroleum industry's upstream budget has been apparent in recent decades. However, even with the discovery of 42 giant fields (>500 million BOE), deepwater E&P remains an immature avenue in the oil and gas industry in terms of proven and economical technologies (Weimer et al., 2004). The practicality of using fixed production platforms, such as jacket platforms and jack-up rigs, is greatly hampered by the extreme depths that deepwater projects can reach. It becomes increasingly difficult for a fixed structure to transmit lateral forces (i.e. shear and bending forces) to the seabed as the water depth at which the structure is fixed increases, resulting in the swaying of the topside facility (Lewis, 1982). The costs for such enormous fixed structures also make it uneconomical for usage in deepwater projects (Adrezin et al., 1996). According to Colligan (1999), the overall feasibility of using fixed platforms for offshore production stops just a little bit over 1,000 ft, after which alternatives must be selected. Hence, floating structures such as tension leg platforms (TLPs), FPSOs and spars are used in place of fixed structures. These structures are able to yield or move in response to the lateral wind and wave loads on the structure, reducing the transmission of the total loads to the seabed. In order to achieve this sort of response, these floating structures need to be secured on location via dynamic systems such as catenary or taut leg mooring with the use of anchors. This requires anchors to 'nail' one end of each mooring line to the seabed which will attenuate both vertical and lateral loads acting on the floating structures as tension builds up in the mooring lines, allowing the structure to move within a fixed design boundary. The anchors used can be further categorized into suction anchors, vertically loaded anchors (VLA), suction embedded plate anchors (SEPLA) and torpedo anchors, depending on their respective working principles and installation methods.

1.2 PROBLEM STATEMENT

It is well-known that the installation method of the torpedo anchor, introduced in 1996, is less sophisticated as compared to other deepwater anchors used in the petroleum industry. Over 60 finned and finless torpedo anchors of various sizes and weights have been field-tested in recent years. However, due to large penetration depth variations obtained by practitioners, torpedo anchors still require more comprehensive testing and full-scale installations of prototypes to increase the confidence of the petroleum industry in this innovative concept (Colliat, 2002). Deployed torpedo anchors that have excessive inclination after penetration have been known to be retrieved and redeployed due to its reduced holding capacity (Raie & Tassoulas, 2009). While there is no standard design manual for torpedo anchors, the effect of the torpedo anchor's length on its eventual holding capacity still has not been explored thoroughly.

1.3 OBJECTIVE

This project aims to:

- a) To evaluate the vertical holding capacity of torpedo anchors using analytical and numerical methods
- b) To analyze the correlation between the length of a torpedo anchor and its holding capacity

1.4 SCOPE OF STUDY

This project concentrates on the correlation between the vertical holding capacity of torpedo anchors at different total lengths. The parameter that is investigated in this project is the total length of the torpedo anchor and how it responds to loads applied to it at an angle of 90° or vertical at the top end of the anchor. Throughout the course of this study, no hydrodynamic effects are considered. The soil is modelled as a homoeogeneous, isotropic linear elastic medium

CHAPTER 2

LITERATURE REVIEW

2.1 SUCTION PILES/ANCHORS

The suction pile or anchor greatly resembles an inverted cup; where one end is close and the other is open (Wang et al., 1978). The anchor is made of a reinforced hollow cylinder which acts as the penetration skirt, and is equipped with a pump, a porous plate and valves. Its cylindrical shell usually has a length to diameter ratio in the range of 5 to 7 with diameters of 8 to 24 ft (Ehlers et al., 2004). The cover plate can be designed to be retrievable or permanent depending on the vertical load requirements. While the anchor's weight and suction is sufficient for installation in cohesive soils, additional weights are needed to increase penetration of suction anchors in cohesionless soils.

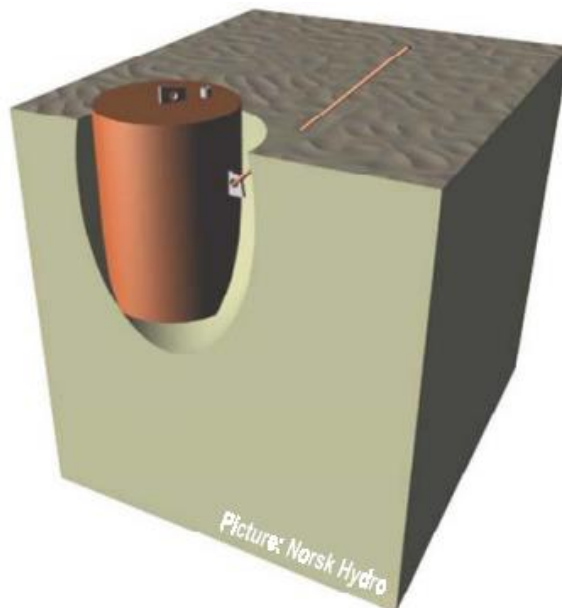


Figure 2.1: Suction pile with taut leg mooring (Sparrevik, 2002)

The suction anchor is installed by inducing differential pressures between the interior of the cylindrical shell and the region surrounding it by means of pumping water out of the interior (Ehlers et al., 2004). Installation begins by lowering the suction anchor

to some degree of penetration in the seabed due to its self-weight before pumping water out of the shell. This results in the hydrostatic pressure outside the shell to be higher than the reduced pressure inside, providing a pressure difference that will drive the anchor into the soil in addition to its weight (Andersen et al., 2005). Mooring loads on the anchor are usually applied to an external padeye on the body of the shell. Design calculations are carried out to position the load attachment point (external padeye) such that the applied mooring load and the soil reaction forces are balanced, and the anchor fails only by translation (Sparrevik, 2002). Due to this the maximum holding capacity of a suction anchor is usually achieved in translational mode of failure.

Since its introduction, the suction anchor has been revered for its simplicity in accurate installation (Ehlers et al., 2004). Being the most experienced deepwater mooring anchor has led to ever more refined design and installation procedures. Moreover, any disorientations or misalignments in its installation can be easily corrected through the direct retrieval of the suction anchor (Senpere & Auvergne, 1982).

The suction anchor's sheer size and weight may require the rental of a crane vessel and require more trips to and from shore to deploy the designed number of anchors (Ehlers et al., 2004). Its installation also cannot be done without the use of an ROV. In terms of design, the suction anchor has reduced efficiency in cohesionless soils (Eltaher et al., 2003). According to Ehlers et al. (2004), the design of a suction anchor requires advanced testing techniques to acquire accurate soil data since these anchors are known to have problems with holding capacity when installed in layered soils.

2.2 VERTICALLY LOADED ANCHORS (VLA)

Vertically loaded anchors (VLA) can be employed, with an angle of 35 to 45 degrees between the seabed and mooring lines, for taut leg mooring applications used in offshore structures (Huang & Lee, 1998). The VLA essentially comprises of two parts namely the shank and fluke, the latter of which it derives its holding capacity

from. Available VLAs on the market include the Bruce Denla and the Vryhof Stevmanta.

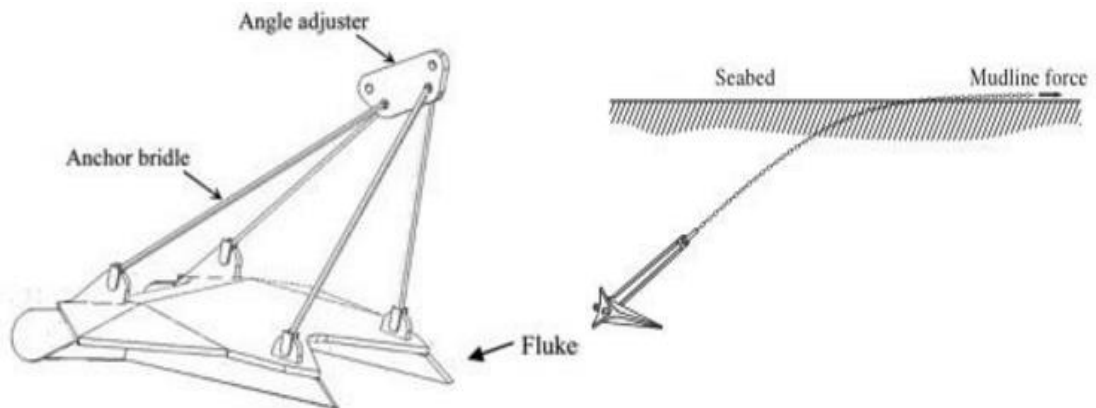


Figure 2.2: Schematic of Vryhof Stevmanta (left) and Anchor drag installation (right) (Murff et al., 2005)

Installation of a VLA is similar to that of a conventional drag embedment anchor in which both anchors are required to be towed by an anchor handling vessel (AHV) in order to penetrate into the seabed. Installation begins by lowering the VLA to the seabed with its fluke, which is essentially a large bearing plate, pointing towards the seabed as it lands. The angle between the fluke and the shank upon landing on the seabed depends on the soil type. The AHV then drags the anchor, transmitting the load to the fluke through the rigid bar-like shank or bridle, causing the anchor to penetrate towards the design depth below the seabed (Ehlers et al., 2004). When the monitored tension reaches the predetermined cable tension, the shank is triggered via shearing at the angle adjuster as shown in Figure 2.2 to allow the anchor line load to achieve an approximately normal position with respect to the fluke (Murff et al., 2005). This change in orientation between the shank and the fluke will improve the holding capacity of the anchor by 2.5 to 3 times relative to the installation load. Before being attached to the floater, the AHV increases the cable tension until the anchor's proof tension load is achieved.

Due to the VLA being lightweight and small in size, the transportation time to conduct a full anchor spread is reduced. As is the case for suction anchors, VLAs also possess the advantage of well-developed design and installation procedures (Ehlers et al., 2004).

The complex installation method which involves the dragging, keying and proof loading of a VLA requires multiple vessels and an ROV to be completed (Ehlers et al., 2004). The lack of a monitoring system to track and assure that the anchor has been installed at design penetration depth also puts the VLA at a disadvantage for application. Moreover, as noted by Ehlers et al. (2004), VLAs only working experience with permanent floating structures are within Brazilian waters.

2.3 SUCTION EMBEDDED PLATE ANCHOR (SEPLA)

The suction embedded plate anchor (SEPLA) puts into practice the concepts of the suction anchor and the vertically loaded anchor (VLA) simultaneously. The SEPLA consists of a rectangular fluke and a full-length keying flat mounted along the top edge of the fluke using an offset hinge. Due to the hinge used, soil pressure along the flap's top edge will force it to rotate about the fluke which will increase the vertical end bearing area by four times (Wilde et al., 2001). This will avoid the SEPLA from translating back up its installation track when a tension load is applied to it.

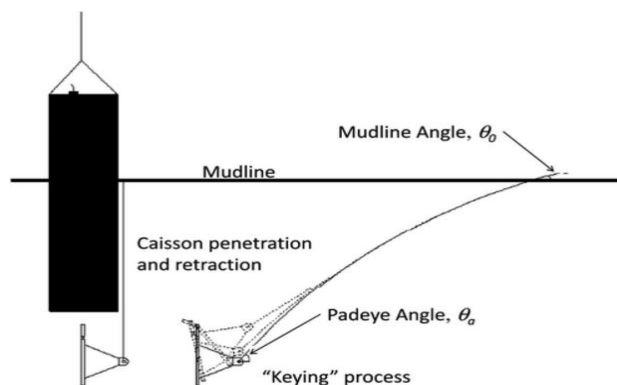


Figure 2.3: Schematic of SEPLA installation (Yang et al., 2011)

Installation of the SEPLA integrates the use of differential pressure for penetration and 'keying' or repositioning of the fluke before proof loading. The SEPLA requires a suction pile, otherwise called a suction follower in this case, in order to achieve design penetration (Wilde et al., 2001). Prior to being lowered to the seabed, the SEPLA is vertically slotted into the base of the suction follower and held in place by the mooring line. As the resistance of the soil on the suction follower equals the follower's weight, the vent valve is closed and the pumping of water out of the follower is carried out, creating a differential pressure and subsequently driving the follower to its design penetration (Yang et al., 2011). The pumping process is reversed and water again fills up the follower before being removed vertically,

leaving the SEPLA in place. It is then rotated or ‘keyed’ as the AHV applies a tension load on the mooring line connected to the SEPLA’s offset padeye, ultimately achieving a perpendicular orientation relative to the applied load where the SEPLA’s holding capacity takes effect.

Other than integrating the use of the proven suction installation method, the SEPLA’s anchor element is also the cheapest to produce among all deepwater anchors (Ehlers et al., 2004). The position and penetration of the anchor plate part of the SEPLA is also able to be determined accurately. Its design procedure is also based on proven design methods of plate anchors.

The main disadvantage of the SEPLA is that it is a proprietary installation method; which contributes to its limited applications in real time mooring (Ehlers et al., 2004). Also, according to Ehlers et al. (2004), the installation of a SEPLA will take about 30% more time as compared to a conventional suction anchor, partly due to the need for keying and proof loading.

2.4 TORPEDO ANCHORS

The torpedo anchor was introduced in 1996 as an alternative anchor concept to provide vertical load bearing capacity. In essence, a torpedo anchor is a cylindrical pipe section with a conical tip and a padeye on top (Raie & Tassoulas, 2009). Fins are also added to the anchor’s cylindrical shell in order to improve directional stability during installation (Hasanloo & Yu, 2011). The anchors are filled with high-density materials such as metal, concrete and scrap chain.

The installation of a torpedo anchor is based on the concept of free fall. It does not require any external source of energy to penetrate the seabed and has a quick installation process. The torpedo anchor is lowered while being connected to two cables where one cable is the permanent mooring cable while the other is a temporary cable (Ehlers et al., 2004). After the anchor is lowered to its pre-determined free fall height, either one of the cables releases it to penetrate the seabed under its own weight. An ROV is also used for pre-drop and post-drop monitoring (Lieng et al., 1999).

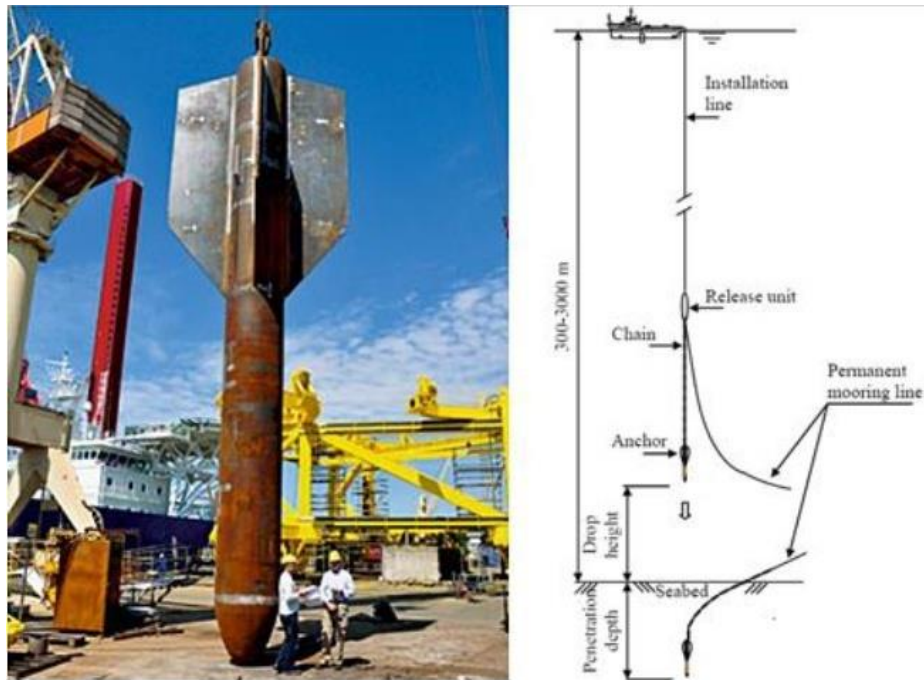


Figure 2.4: Full scale torpedo pile and releasing situation (Lieng et al. 1999)

The main advantage of the torpedo anchor is its simplicity in design, being able to practice the API RP 2A guidelines as used in conventional pile design procedures (Ehlers et al., 2004). Its compact and robust design is simple and cost effective to fabricate. The filling of the centre core and completion assembly can also be performed en route to its installation site since no surface coating is required for the anchor (Lieng et al., 1999). Due to its working principle, the installation of torpedo anchors are simple and cost effective; where one vessel and ROV each are able to complete the task (Ehlers et al., 2004).

The main disadvantage of the torpedo anchor is that it is a proprietary installation method; which contributes to its limited applications in real time mooring to Brazilian waters alone (Ehlers et al., 2004). Also, according to Ehlers et al. (2004), the lack of properly documented design and installation steps, and monitoring systems for post-installation verticality are also problems faced by users of torpedo anchors.

2.4.1 Previous Work

Much of the previous researches carried out by the intellectual society have been focused on the installation procedure and holding capacity of the torpedo anchors in various soil conditions. Hossain et al. (2014) reported that the anchor embedment depth and impact velocities increase with increasing drop height and decreasing soil shear strength. It was also revealed that the cavity above the anchor post-installation is critical in augmenting the downward anchor load during installation and increases reverse bearing and skin friction along the anchor surface. The anchor's holding capacity was also found to increase with increasing post-installation consolidation time, anchor embedment depth, soil undrained shear strength and reduced angle between the pullout load and mudline. On the topic of geometry, Hossain et al. (2014) concluded that the normalized holding capacity of their Model B (vertical fins and conical tip) was about 1.3 times that of Model N (butterfly vertical fins and ellipsoidal tip).

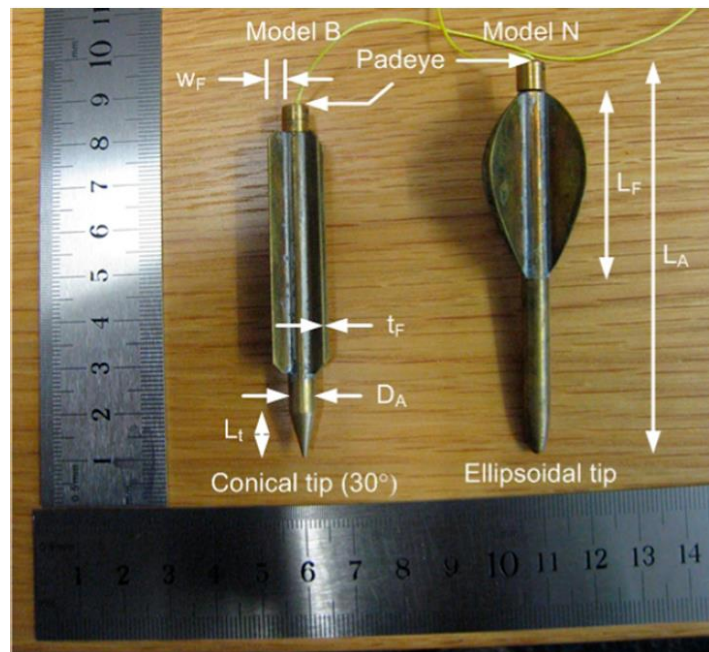


Figure 2.5: Model B (left) and Model N (right) used in centrifuge test (Hossain et al., 2014)

Raie and Tassoulas (2009) used computational fluid dynamics (CFD) simulation, modelling soil as a viscous fluid, to predict the torpedo anchor's penetration depth and estimate the shear and pressure distributions along the anchor-soil interface. Sturm et al. (2011) conducted a quasi-static simulation of the torpedo anchor installation process using the finite element (FE) method and found that the penetration depth of the anchor is highly affected by soil profiles with varying shear

strengths. For their considered cases, the pure vertical holding capacity of the anchor is not only unaffected, but may be even higher if the softer layers of soil are covered with stiffer layers and the flukes of the anchor are positioned in the stiffer soil.

Lieng et al. (2000) carried out a 3D FE analysis and design calculations estimated from API techniques in their efforts to optimize the design of a deep penetrating anchor. It was concluded that the design load of the anchor will be its maximum vertical load as they have shown that there is ample horizontal load capacity. de Sousa et al. (2011) also conducted a 3D FE analysis to investigate the effects of load inclination with respect to the plane of the flukes, soil parameters and number of flukes on the long term undrained holding capacity of torpedo anchors. They concluded that the soil parameters and number of flukes of the anchor are important in determining its holding capacity while the load inclination does not significantly affect the anchor's holding capacity.

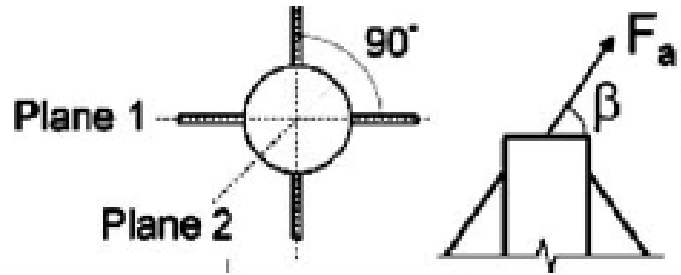


Figure 2.6: Direction of load applied to the anchor and the two planes used to measure effect of load inclination with respect to fluke planes (de Sousa et al., 2011)

Despite all the research done in investigating the holding capacity and penetration depth of torpedo anchors, the fundamental geometries like diameter and length have never been acknowledged. Therefore, more emphasis should be put on the design of the anchor itself to compliment the widespread research in order to utilize this technology to its fullest extent.

2.5 LOAD BEARING CAPACITY OF PILES

Piles are structural members used in deep foundations and are usually made of steel, concrete and timber. The ultimate load-bearing capacity of a pile, Q_u , is defined as the summation of the load-carrying capacity of the pile point, Q_p , and the shaft frictional resistance, Q_s (Das, 2012).

$$Q_u = Q_p + Q_s \quad [1]$$

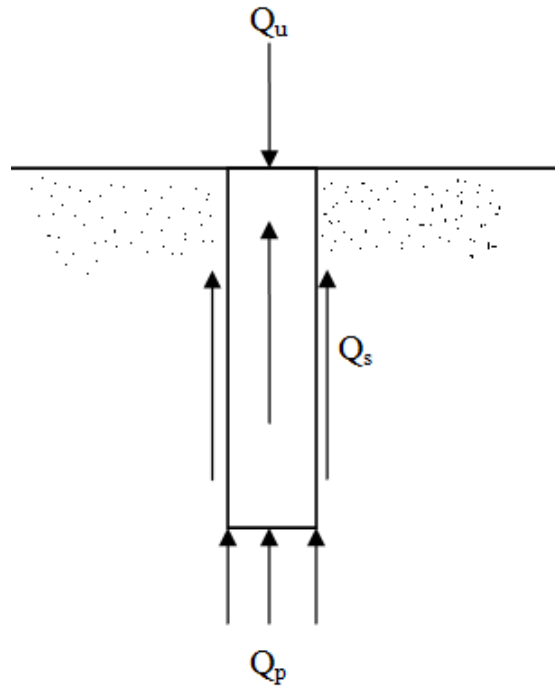


Figure 2.7: Load and reaction forces a pile

2.5.1 Load-Carrying Capacity of the Pile Point, Q_p

The ultimate bearing capacity of a pile is usually expressed as

$$q_u = c'N_c^* + qN_q^* + \gamma BN_y^* \quad [2]$$

where the necessary shape and depth factors determine the bearing capacity factors N_c^* , N_q^* and N_y^* . An equation whose form is similar to that of Equation 2 may be used to express the load-carrying capacity per unit area of the pile point, q_p , albeit with different bearing capacity factors. Substituting the width of the pile, D_p , for B in Equation 2

$$q_u = q_p = c'N_c^* + qN_q^* + \gamma D_p N_y^* \quad [3]$$

The third term in Equation 3 may be omitted as the width of the pile is usually a relatively small value. Equation 3 then becomes

$$q_p = c'N_c^* + q'N_q^* \quad [4]$$

The term q has been replaced by q' to represent effective vertical stress. Therefore, the load-carrying capacity of the pile point is the product of the surface area of the pile tip, A_p , and the vertical stress applied onto the pile, q_p . Multiplying Equation 4 with A_p ,

$$Q_p = A_p q_p = A_p (c' N_c^* + q' N_q^*) \quad [5]$$

According to Meyerhof's method, the load-carrying capacity of a pile point in saturated clays in undrained conditions, where c_u = undrained cohesion of the soil below the pile tip, can be calculated as

$$Q_p = N_c^* c_u A_p = 9 c_u A_p \quad [6]$$

2.5.2 Frictional Resistance, Q_s

According to Das (2012), frictional skin resistance of a pile can be expressed as

$$Q_s = \sum p \Delta L f \quad [7]$$

where p = perimeter of the pile section

ΔL = incremental pile length over which p and f are taken constant

f = unit friction resistance at any depth z

The α method states that the unit skin resistance in clayey soils can be represented by the equation

$$f = \alpha c_u \quad [7]$$

where α is the empirical adhesion factor approximated from its relation with the undrained cohesion, c_u , as shown in Figure 2.8.

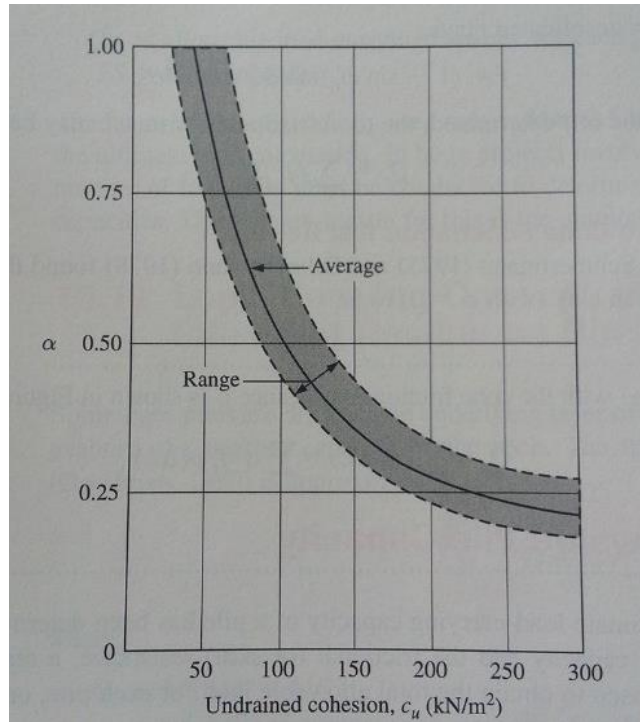


Figure 2.7: Variation of α with c_u (Das, 2012)

Thus, the frictional resistance in clay can be expressed as

$$Q_s = \sum p\Delta Lf = \sum \alpha c_u p\Delta L \quad [8]$$

The working principle or anchoring mechanism of torpedo anchors is very similar to that of the pile as explained previously. The only difference being that the Q_u , Q_p and Q_s act in the opposite directions as the anchor resists pullout instead of compression loads.

CHAPTER 3 METHODOLOGY

3.1 PROJECT WORK & FLOWCHART

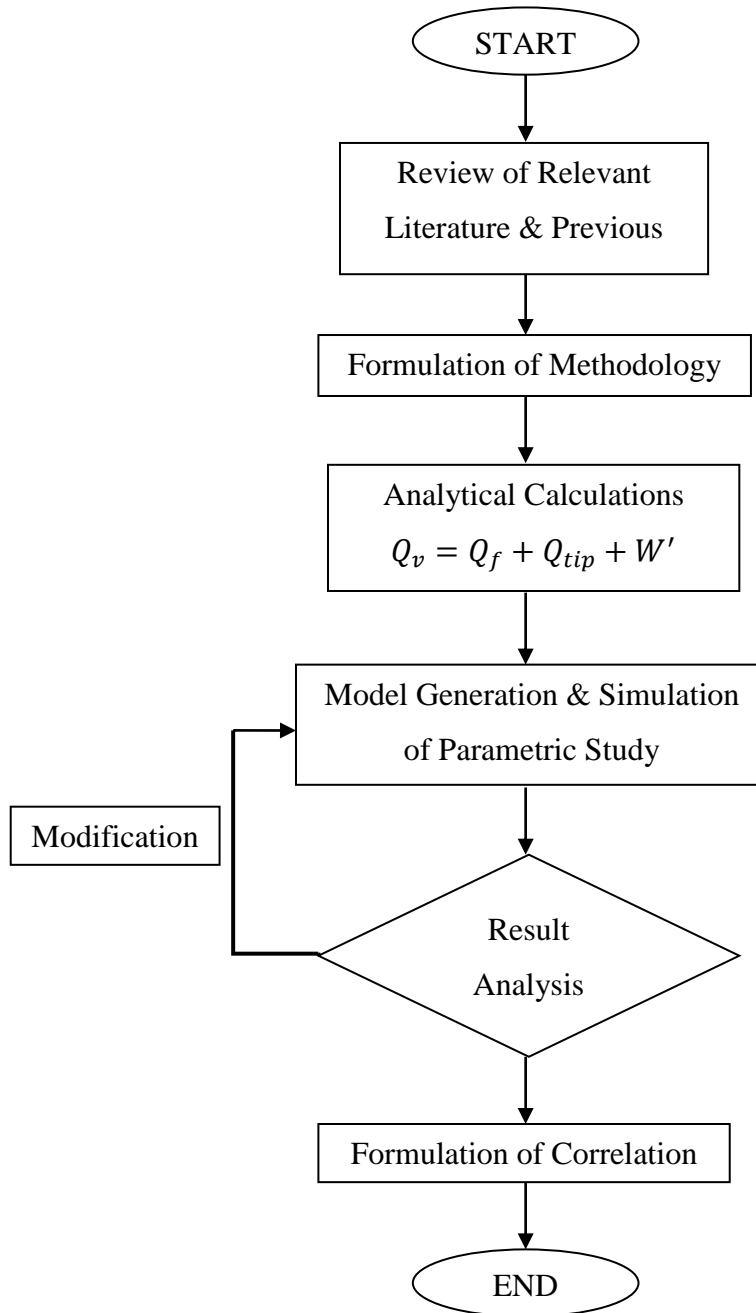


Figure 3.1: Flow of project tasks

The project consists of two major parts: the analytical calculations and the finite element (FE) simulation of the torpedo anchor holding capacity. Each part will be explained in further detail in subsequent sub-topics.

3.2 ANALYTICAL CALCULATIONS

Analytical calculations will first be carried out to determine the theoretical vertical holding capacity of torpedo anchors of different lengths. Results from these calculations will then be used to compare to the results obtained from the finite element model.

3.2.1 Formula

The pullout of a torpedo anchor is in many ways similar to a tension loaded pile as mentioned in the previous chapter. Hence, the equation used to compute the total vertical pullout capacity of torpedo anchors is similar to Equation 1; with the addition of a new W' term to represent the anchor's submerged weight. As presented by Lieng et al. (2000), the vertical holding capacity can be expressed as

$$Q_v = Q_f + Q_{tip} + W' = \tau_{vn} \cdot A_{wall} + q_{av} \cdot A_{tip} + W' \quad [9]$$

where

$$\tau_{vn} = \alpha \cdot s_u \quad [10]$$

$$\alpha = 0.5(s_u/p'_o)^{-0.5} \text{ for } s_u/p'_o \leq 1 \quad [11]$$

$$q_{av} = N_c s_u \quad [12]$$

3.2.2 Anchor Geometry

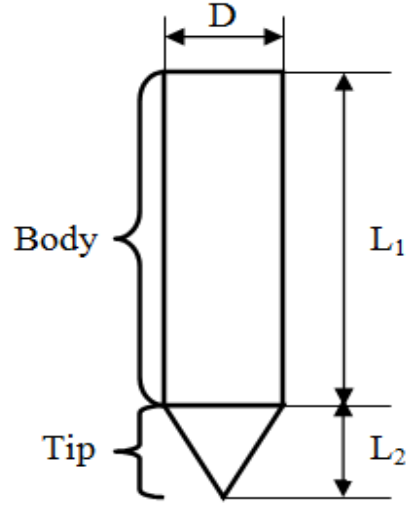


Figure 3.2: Schematic representation of the torpedo anchor and its relevant dimensions

For the purposes of this project, a finless torpedo anchor is assumed. It consists of a cylindrical body and a conical tip, both sharing the same diameter, D . The total length of the anchor, L_{total} , is the sum of the length of the anchor body, L_1 , and the length of the conical tip, L_2 . Throughout all variations in the total length, the ratio of $L_1:L_2$ is assumed to be 4:1.

The total surface area of the anchor can be calculated from surface area equations for cylinders and cones. For the both the anchor body and tip, only the curved surfaces and one circular base of the body are taken into account for the purpose of the analytical calculations. Hence, the two circular areas where the base of the conical tip and cylindrical body meet are not exposed to the surroundings and are subsequently omitted from the calculations of surface area.

Then, the surface area terms A_{wall} and A_{tip} , as required by Equation 9, can be expressed as

$$A_{wall} = \pi D L_1 \quad [13]$$

$$A_{tip} = \frac{\pi D}{2} \sqrt{(L_2)^2 + \left(\frac{D}{2}\right)^2} + \frac{\pi D^2}{4} \quad [14]$$

3.2.3 Parameters

To conduct the analytical calculations, a certain number of parameters must first be defined. They are the anchor parameters and soil parameters, both of which can be seen in the table below.

	Parameter	Value
Anchor	Lengths	10 m, 13 m, 15 m, 17 m, 20 m
	Diameter	1.0 m
	Mass	100 tons
Soil	Undrained shear strength, s_u	18 kPa
	Saturated specific weight, γ_{sat}	19 kN/m ³
	Bearing capacity factor, N_c	21.75

Table 3.1: Relevant parameters used in analytical calculation of torpedo anchor holding capacity

It is important to note that all anchor parameters were arbitrarily assigned after review of torpedo anchor field test data while the soil parameters were calculated from the average values of the respective parameters as given by geotechnical engineering agencies on their company websites. The soil values recorded were for very soft to medium soft clays, depending on availability of data required.

3.3 FINITE ELEMENT (FE) MODELING

The finite element analysis is done using a 2D axisymmetric model made up of two bodies namely the soil and the anchor. The analysis is conducted as a large displacement multi-body static analysis using ‘initial contact’ bonded contact elements with an arbitrary friction coefficient of 0.2 at the interface. ANSYS Mechanical APDL is used in the analysis.

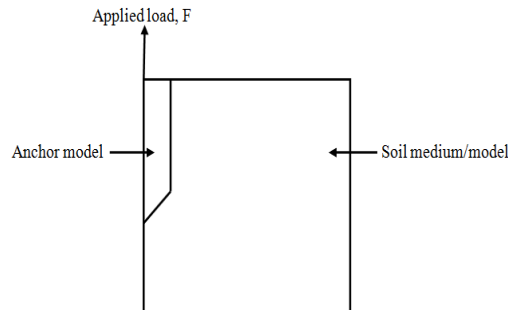


Figure 3.3: Schematic of FE model

3.3.1 Soil

The soil medium is modelled as a homogeneous, isotropic linear elastic using higher-order 2D, 8-node elements. The overall dimensions of the area are 10m width and 25m height, with a pocket where the anchor body fits into. Hence, the dimension of the pocket changes according to the dimensions of the anchor.

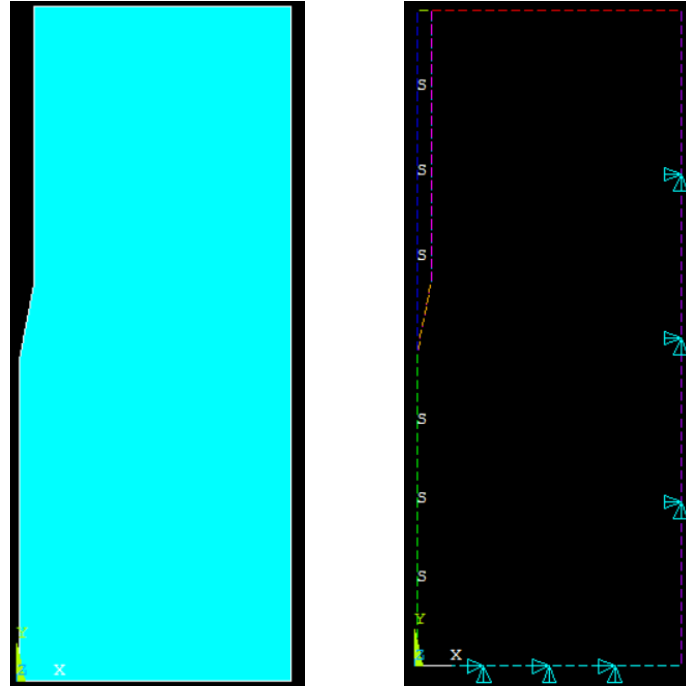


Figure 3.4: Area of soil body (left) and constraints applied onto soil body (right)

According to the analytical calculations, the soil is assumed to be in undrained conditions, which means that the pore water between soil particles are not allowed to drain out of the volume. This disallows pore pressure relief and keeps the pressure generated by the compressed water within the volume of the soil.

In order to induce this undrained condition of the soil, the model's displacement is restrained in the vertical or Y direction at the base and in the horizontal or X direction on the outer(right) wall (de Sousa et al., 2011). This is sufficient to simulate the undrained conditions of the soil as it does not allow pore pressure relief via movement of the soil and subsequent volume expansion. Besides that, a symmetry displacement boundary condition is also applied on the outer left wall of the soil, which is the centre of the soil volume if the area is revolved about the y axis.

Parameter	Value
Density	1750 kg/m ³
Young's Modulus, EX	8500 kPa
Poisson's Ratio, PRXY	0.45

Table 3.2: Properties of soil model

3.3.2 Anchor

The anchor is also modelled as a homogeneous, isotropic linear elastic material using the same elements used for the soil. The overall lengths vary as stated previously. Three length cases are considered: 10m, 13m and 15m respectively. The diameters of the anchor in these three cases remain constant at 1.0m.

In order to isolate the length as a parameter to be measured, all other parameters that are not related to the length of the anchor are held constant. Hence, the density assigned to the anchor for all three cases are different due to their changing geometry and assumed constant mass of 100 tons. This is important as the simulation of the model requires the initiation of gravitational acceleration to induce penetration of the anchor into the soil. Applying the same density value for all cases will result in different values of mass due to their different volumes.

Parameter	Value
Density	variable
Young's Modulus, EX	200 GPa
Poisson's Ratio, PRXY	0.3

Table 3.3: Properties of anchor model

3.3.3 Contact

Multi-body analyses such as this require the use of contact elements at the interface between the interacting bodies. This is so the responses of the bodies become dependent and are able to simulate real world phenomena. As a general rule of thumb, the stiffer body between two is usually chosen as the target while the other is assigned as the target. In this problem, the anchor is the stiffer of the two bodies. Hence, the outer surface of the anchor is layered with target elements while the outer surface of the soil is layered with contact elements (de Sousa et al., 2011). This will

enable interaction between bodies despite the load being applied only to one, so long as the target and contact elements are in the active state.

The chosen type of contact is the surface-to-surface, bonded (initial contact) available in the ANSYS contact library. This contact assumes initial contact between the two predicted interacting bodies before any loads are applied to the system. Once loads are applied to any one body, the contact allows relative movement in the form of sliding and gaps. An arbitrary frictional coefficient of 0.2 is assumed in this problem.

3.3.4 Load Step

The solution to this problem requires two load steps to be simulated, one at a time. Since the installation of the torpedo anchor is not considered in this problem, the anchor will have to be ‘wished in place’. Hence, the first load step is the gravity load step where a global gravitational acceleration is applied to the system. At the completion of this step, an initial stress state will have been induced between the soil and the anchor. The application of gravitational acceleration does not require any substep settings.

Secondly, the vertical pullout load is applied. The load is applied at the top left vertex of the anchor which is the centre of the anchor since the external padeyes or mooring lines which are supposed to be connected to the anchor are not modelled (de Sousa et al., 2011). This second load step is repeated until a failure, defined as the undrained shear strength (18kPa) used in computing the vertical holding capacity as mentioned in the previous section, is obtained between the body of the anchor and the soil in contact with it.

3.4 GANTT CHART

No.	Activities Weeks	FYPI														FYPII																								
		1	2	3	4	5	6	7	8	9	10	11	12	13	14	1	2	3	4	5	6	7	8	9	10	11	12	13	14											
1	Literature review																																							
2	Familiarize with ABAQUS software																																							
3	Define parameters of simulation																																							
4	Calculation of preliminary analytical results																																							
5	Modeling of soil, anchor & contact surfaces																																							
6	Simulation of holding capacity																																							
7	Analysis of simulation results																																							
8	Preparation of relevant paper work																																							
		● denotes key milestone																																						

CHAPTER 4

RESULTS AND DISCUSSION

4.1 ANALYTICAL CALCULATIONS

The analytical calculations as discussed in Chapter 3 were carried out using Microsoft Excel worksheets. The calculations were done based on the lengths of the torpedo anchors ranging from 10m to 20m, with an interval of 0.5m. Parameters of interest including the holding capacity, wall area of the torpedo anchor and the tip area of the torpedo anchor.

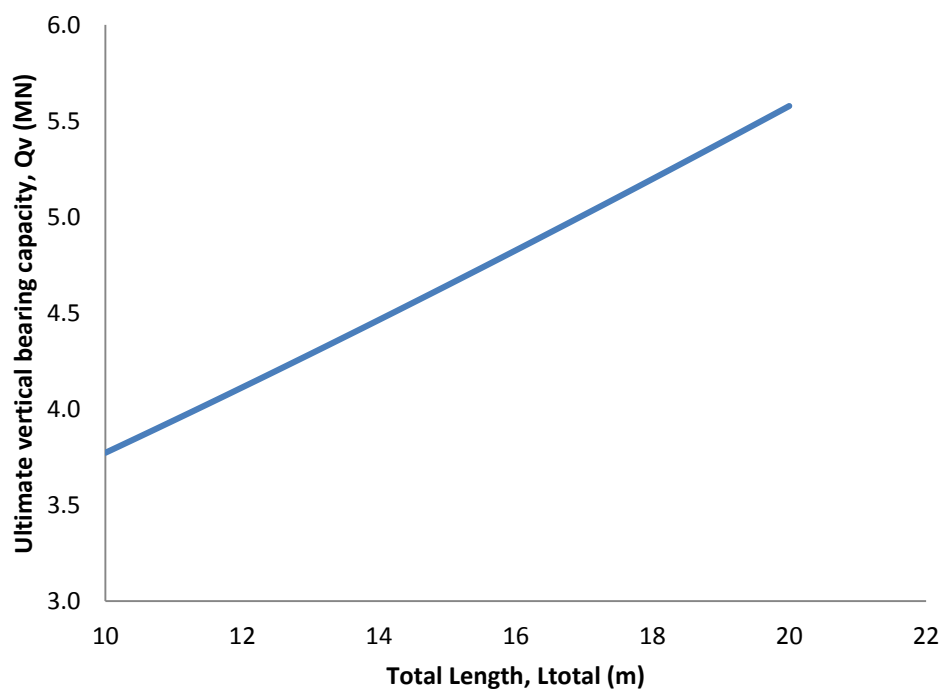


Figure 4.1: Graph of vertical holding capacity versus total length of torpedo anchor

From the calculations done, it can be seen that the vertical holding capacity of a torpedo anchor increases linearly with increasing total length. From the gradient of the line of best fit, it is shown that the holding capacity increases at a rate of 0.18MN per 1m increase in the total length of the torpedo anchor.

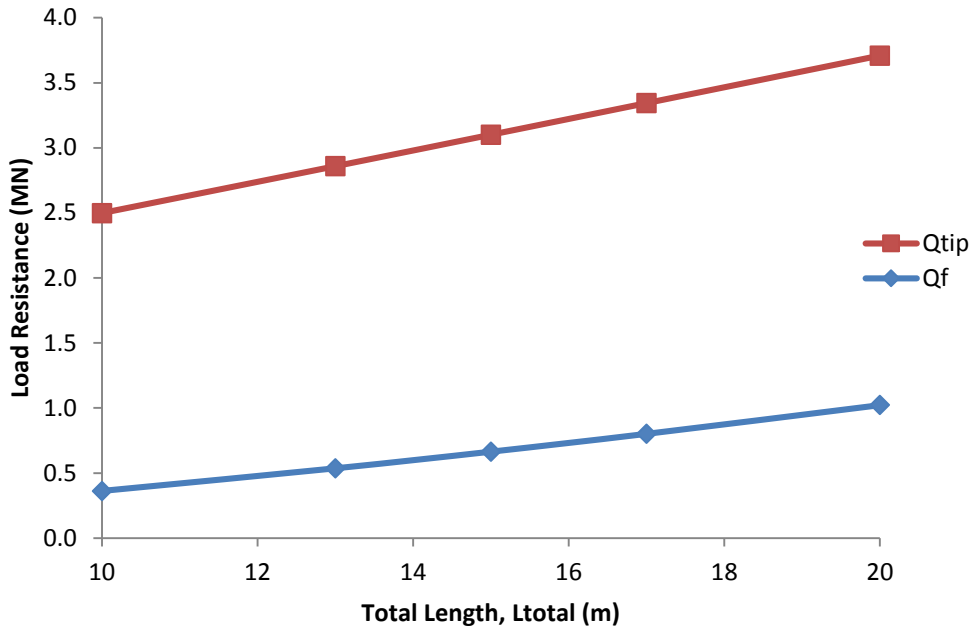


Figure 4.2: Graph of load resistance versus total length of torpedo anchor

The increase in the torpedo anchor's holding capacity is attributed to the increase of both the tip and friction resistance as the total length of the anchor increases. Although both the tip and friction resistances increase, it is important to note that the tip resistance is always much larger than the friction resistance. On average, the tip resistance is about 2.4MN greater than the friction resistance at every length.

While both types of unit resistances, τ_{vn} and q_{av} , are dependent on the undrained shear strength of the soil, the coefficients multiplied to the undrained shear strength are different. The adhesion variable is used for the unit friction resistance whereas the constant bearing capacity factor is used for the unit resistance of the tip.

The adhesion coefficient is a variable dependent on the total length of the torpedo anchor. Although the value of it increases with increasing total length, its increment magnitude is small. In this data set, the adhesion coefficient ranges from 0.8 to 1.13.

The bearing capacity factor, on the other hand, is a large constant coefficient. The value used in this data set is 21.75. Hence, the unit tip resistance remains at a constant value of 391.5 kPa, which is much larger than the unit friction resistance.

Figure 4.3 shows the relation between the wall and tip surface area with increasing total length. The wall and tip surface area are used in the calculation of the total friction resistance and total tip resistance of the torpedo anchor as shown in Equation 9. Even as the value and increment rate of the wall surface area is always greater than that of the tip surface area, the gap between the two values is small in comparison to the gap between the unit tip resistance and unit friction resistance. Thus, mathematically, the total tip resistance of a torpedo anchor will always be greater than the total friction resistance within a reasonable range of the anchor length.

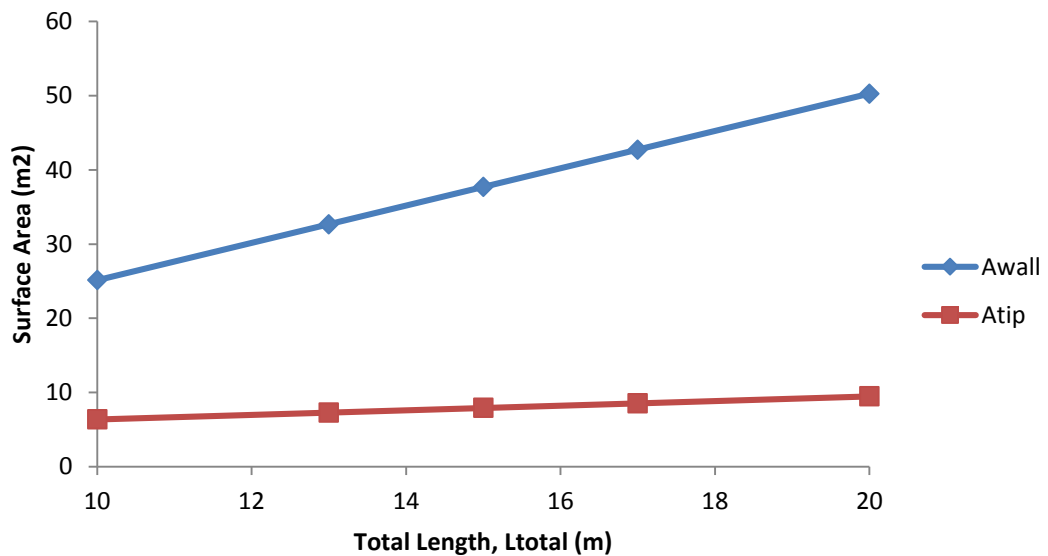


Figure 4.3: Graph of surface area versus total length of torpedo anchor

From the physical point of view, as the torpedo anchor penetrates the seabed, it creates a negative differential pressure at the top end of the anchor causes the hole created by the penetration to collapse (Lieng et al., 2000). This then causes the soil to completely engulf the anchor. Thus, if the anchor were to fail by shear, it would first require a load large enough to displace the soil that collapsed onto the top end of the anchor or by displacing a large amount of soil as the anchor rotates due to the lateral loads causing the soil surrounding the wall to fail. However, more research needs to be done on the latter case as that particular mode of failure does not exhibit a clear holding capacity (de Sousa et al., 2011).

4.2 FINITE ELEMENT (FE) MODELING

Due to the time constraint and unexpected technical issues with the software, simulations were only completed for the cases of 10 m, 13 m and 15 m total length of the torpedo anchor.

The undrained shear strength of the soil used in the analytical calculations is assumed as the failure criterion. Unlike actual soil, the modelled soil will not undergo plastic deformation as shown by its behaviour in Figure 4.4.



Figure 4.4: Stress-strain curve of an isotropic linear elastic material (Atkinson, n.d.)

This means that, in real time, the surface of this soil model would never be detached from the surface of the anchor until the anchor's surface has displaced outside the limits of the soil model's original shape. With this knowledge, a failure gap or relative displacement between the two bodies would be unreasonable.

This is also why the analysis involves only two bodies instead of the conventional three used in torpedo anchor holding capacity problems. In conventional problems of holding capacity as pursued by Lieng et al. (2000), de Sousa et al. (2011) and Pecorini & De (2015), on top of the soil and anchor bodies, there is a third body representing the soil at the anchor position. Only with the third body is it possible to induce an initial stress state within the soil. However, using a homogeneous,

isotropic linear elastic material, it is unnecessary as the soil model will not undergo plastic deformation.

Three length cases have been simulated with acceptable results. The 10m model is shown with the Von Mises stress contour after the gravity load in Figure 4.5.

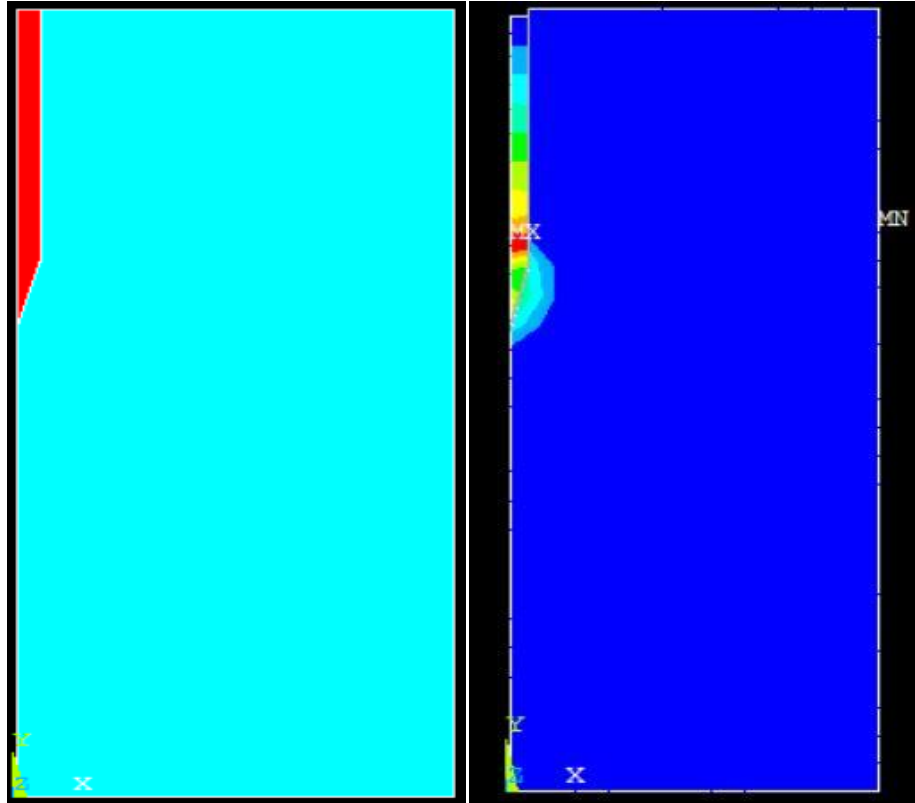


Figure 4.5: Soil-anchor model (left) and Von Mises stress contours after gravity load (right)

As mentioned in the previous chapter, the simulation of the anchor pullout is repeated with different magnitudes of load until a shear stress of more than 18kPa is generated in the region along the anchor body. In Figure 4.6, it is shown that the minimum shear stress at the expected failure region is 18.6kPa, which surpasses the failure criterion assumed beforehand. Hence, the load at which this situation occurs is assumed to be the vertical holding capacity.

The vertical holding capacity of the 10m, 13m and 15m anchors were observed to be 2.72MN, 3.27MN and 3.53MN respectively. These values were then compared to the values obtained through the analytical calculations to calculate for the percentage difference. The percentages difference obtained were 27.91%, 23.74% and 24.01% respectively.

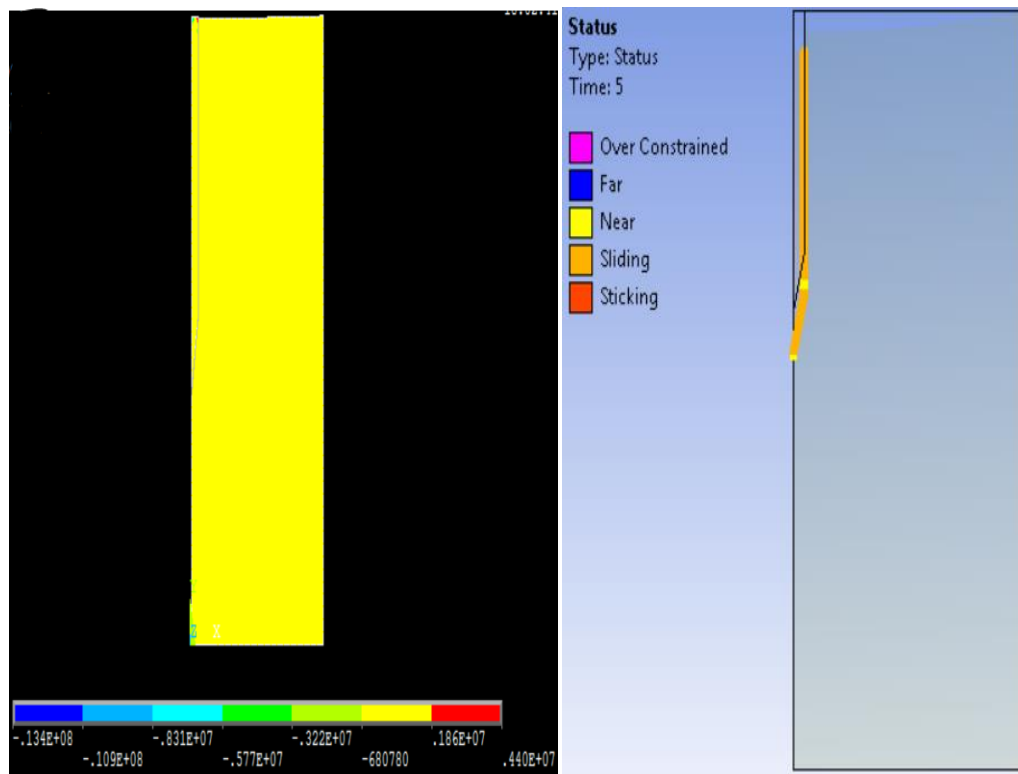


Figure 4.6: Shear stress contours (left) and contact status (right) of the 15m length anchor model at 3.53MN load

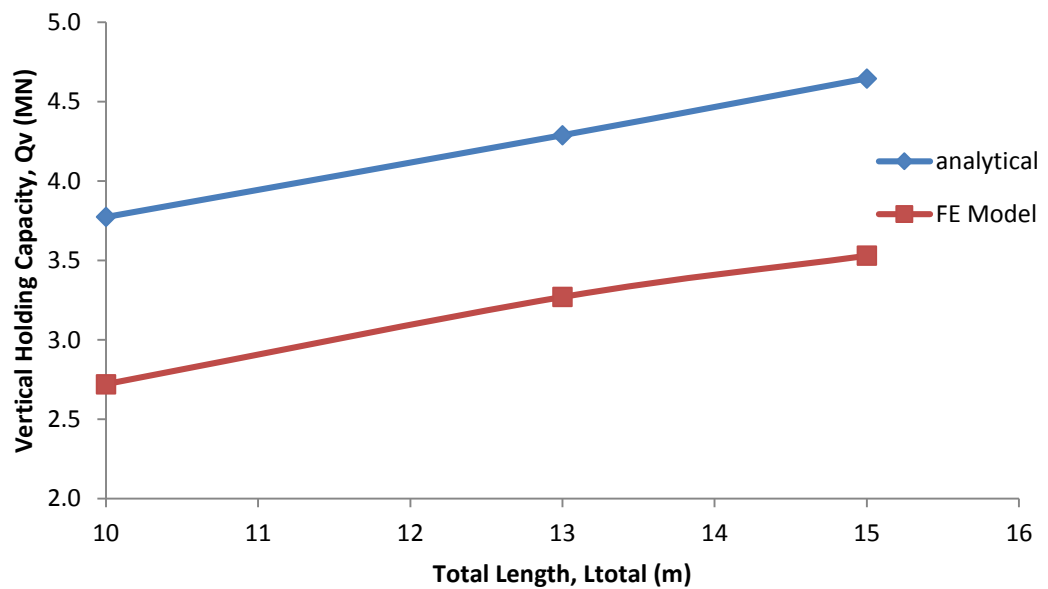


Figure 4.7: Graph of vertical holding capacity versus total length of torpedo anchor for FE model and analytical calculations

However, it is important to note that in the finite element model, there is no part of the soil that collapses onto the top of the anchor since the soil model will elastically deform infinitely as only the Young's modulus is specified. Directly omitting the tip resistance on the top of the anchor, the analytical holding capacities become 2.54MN, 3.06MN and 3.41MN for the 10m, 13m and 15m cases respectively. Recalculating the percentage differences yield the acceptable values 7.09%, 6.86% and 3.52% for the three length cases. Hence, the correlation that is shown by both the analytical and numerical method is that the vertical holding capacity of torpedo anchors increases linearly with the increasing total length of its body.

CHAPTER 5

CONCLUSION AND RECOMMENDATION

Analytical and numerical studies have been conducted to study effect of a torpedo anchor's total length on its undrained vertical holding capacity. The analytical method involves the computation of the anchor's vertical holding capacity at different total length cases. The vertical holding capacity of the anchor is found to increase linearly with increasing total lengths. Besides that, it is also concluded that at any reasonable total length, the load resistance of the anchor tip is always larger than that of the load resistance due to friction on the anchor body. Thus, the vertical holding capacity is the maximum holding capacity of a torpedo anchor.

The numerical study was conducted using a two-dimensional axisymmetric finite element model. Both the soil and anchor were simulated as homogeneous, isotropic linearly elastic materials using plane elements capable of demonstrating non-linearity and large displacement behaviour, where the anchor is significantly stiffer than the soil. Moreover, the interaction between the anchor and soil was represented using contact elements that allow relative sliding and detachment between the two surfaces in contact. The pattern of results obtained from both the numerical model and the analytical calculations agreed upon the premise that the vertical holding capacity of a torpedo anchor increases as the total length of the anchor increases.

It is recommended that persons with intentions to be involved in this particular research topic should attempt to simulate the dynamic conditions and responses of the torpedo anchor via numerical modelling of the anchor's installation before applying the pullout load or through scaled laboratory models. Future works on numerical modelling should also look to apply a material model with properties in closer resemblance to that of soil to achieve more accurate results and correlations. Future researchers may also look into softwares such as PLAXIS or ABAQUS which may provide better functions for solving geotechnical problems such as this one.

REFERENCES

- Adrezin, R., Bar-Avi, P., & Benaroya, H. (1996). Dynamic response of compliant offshore structures-review. *Journal of Aerospace Engineering*,9(4), 114-131.
- Andersen, K. H., Murff, J. D., Randolph, M. F., Clukey, E. C., Erbrich, C. T., Jostad, H. P., ... & Supachawarote, C. (2005, September). Suction anchors for deepwater applications. In *Proceedings of the 1st International Symposium on Frontiers in Offshore Geotechnics, ISFOG, Perth* (pp. 3-30).
- Atkinson, J. (n.d.). *Stiffness*. Retrieved from Universiti of West England website: <http://environment.uwe.ac.uk/geocal/SoilMech/basic/stiffness.htm>
- Colligan, J. (1999). The economics of deep water.
- Das, B. (2012). *Fundamentals of geotechnical engineering*. Cengage Learning.
- de Sousa, J. R. M., de Aguiar, C. S., Ellwanger, G. B., Porto, E. C., Foppa, D., & de Medeiros, C. J. (2011). Undrained load capacity of torpedo anchors embedded in cohesive soils. *Journal of Offshore Mechanics and Arctic Engineering*, 133(2), 021102.
- Ehlers, C. J., Young, A. G., & Chen, J. H. (2004). Technology assessment of deepwater anchors. In *Offshore technology conference*. Offshore Technology Conference.
- Eltaher, A., Rajapaksa, Y., & Chang, K. T. (2003). Industry trends for design of anchoring systems for deepwater offshore structures. In *Offshore Technology Conference*. Offshore Technology Conference.
- Hasanloo, D., & Yu, G. (2011). A Study on the Falling Velocity of Torpedo Anchors during Acceleration. In *The Twenty-first International Offshore and Polar Engineering Conference*. International Society of Offshore and Polar Engineers.

- Hossain, M. S., Kim, Y., & Gaudin, C. (2014). Experimental investigation of installation and pullout of dynamically penetrating anchors in clay and silt. *Journal of Geotechnical and Geoenvironmental Engineering*, 140(7), 04014026.
- Huang, K., & Lee, M. Y. (1998, January). Experiences in classification of deepwater mooring systems for floating installations. In *Offshore Technology Conference*. Offshore Technology Conference.
- Lewis, R. E. (1982). An overview of deepwater compliant structures. In *Annual Meeting Papers, Division of Production*. American Petroleum Institute.
- Lieng, J. T., Hove, F., & Tjelta, T. I. (1999). Deep Penetrating Anchor: Subseabed deepwater anchor concept for floaters and other installations. In *The Ninth International Offshore and Polar Engineering Conference*. International Society of Offshore and Polar Engineers.
- Lieng, J. T., Kavli, A., Hove, F., & Tjelta, T. I. (2000). Deep penetrating anchor: further development, optimization and capacity verification. In *The Tenth International Offshore and Polar Engineering Conference*. International Society of Offshore and Polar Engineers.
- Medeiros Jr, C. J. (2002). Low cost anchor system for flexible risers in deep waters. In *Offshore Technology Conference*. Offshore Technology Conference.
- Merifield, R. S., & Smith, C. C. (2010). The ultimate uplift capacity of multi-plate strip anchors in undrained clay. *Computers and Geotechnics*, 37(4), 504-514.
- Murff, J. D., Randolph, M. F., Elkhatib, S., Kolk, H. J., Ruinen, R. M., Strom, P. J., & Thorne, C. (2005). Vertically loaded plate anchors for deepwater applications. In *Proc Int Symp on Frontiers in Offshore Geotechnics* (pp. 31-48).

- Pecorini, D., & De, A. (2015). Pull-Out Capacity Analysis of Offshore Torpedo Anchors Using Finite-Element Analysis. In *The Twenty-fifth International Offshore and Polar Engineering Conference*. International Society of Offshore and Polar Engineers.
- Raie, M. S., & Tassoulas, J. L. (2009). Installation of torpedo anchors: numerical modeling. *Journal of geotechnical and geoenvironmental engineering*.
- Senpere, D., & Auvergne, G. A. (1982). Suction anchor piles-a proven alternative to driving or drilling. In *Offshore Technology Conference*. Offshore Technology Conference.
- Sparrevik, P. (2002). Suction pile technology and installation in deep waters. In *Offshore technology conference*. Offshore Technology Conference.
- Vryhof Anchors, B. V. (2010). Anchor Manual 2010-The Guide to Anchoring.
- Wang, M. G., Demars, K. R., & Nacci, V. A. (1978). Applications of suction anchors in offshore technology. In *Offshore Technology Conference*. Offshore Technology Conference.
- Weimer, P., Slatt, R. M., & Pettingill, H. S. (2004). Global overview of deepwater exploration and production. *Petroleum Systems of Deepwater Settings*. Tulsa. *SEG/EAGE*, 21-39.